

# Formation of two types of highly luminescent SiO<sub>2</sub> beads impregnated with multiple CdTe QDs

Ping Yang, Masanori Ando and Norio Murase\*

Received (in Durham, UK) 4th June 2008, Accepted 27th October 2008

First published as an Advance Article on the web 1st December 2008

DOI: 10.1039/b809478k

Highly luminescent SiO<sub>2</sub> beads with concentrated CdTe quantum-dots (QDs) stabilized by thioglycolic acid (TGA) have been prepared by using a two-step synthesis including coating the surface of the QDs with SiO<sub>2</sub> and subjecting them to a subsequent inverse micelle process. Two types of bead structures were formed together with a solid structure, depending on the preparation procedures and conditions. The first contains a composite consisting of Cd<sup>2+</sup>, TGA, SiO<sub>2</sub>, and QDs (with egg-yolk structure). This composite was created when highly alkaline water (pH ≥ 10) was added to the solution of surface-coated QDs before a sol–gel reaction occurred in the water droplets though the migration of the content inside the droplets before they solidified. The second contains a void inside of them (hollow structure). This void was formed when highly alkaline water was added after the water droplets had formed. The beads thus prepared demonstrated high photoluminescence efficiency (70%, almost same as the initial colloidal solution) that was maintained for more than a week in water. The lifetime measurement indicates the reduction of non-radiative rate and increment of radiation lifetime of QDs by the SiO<sub>2</sub> coating. The mean concentration of QDs in typical beads was about 0.002 M, where *ca.* 140 QDs were dispersed in all SiO<sub>2</sub> beads 60 nm in diameter.

## Introduction

Semiconductor QDs covalently coupled to biomolecules are expected to be used in biological detection because of their intense luminescence, narrow emission spectral width, and higher stability against photobleaching compared with organic dyes.<sup>1</sup> Coating fluorescent QDs with silica can not only suppress their photodegradation but also impede the release of heavy-metal ions in harsh chemical environments. Furthermore, they can provide a resulting shell that imparts biocompatibility, because the surface of silica can easily be modified with a wide range of functional groups. There have been many reports on encapsulating QDs in silica beads.<sup>2</sup> Normally, only one QD can be embedded in a single bead with a diameter of less than 100 nm. A ligand exchange mechanism has been presented for incorporating of hydrophobic QDs in beads.<sup>2j</sup> To achieve noticeable signal increments in ultra-sensitive bioanalysis, silica beads impregnated with highly luminescent multiple QDs are an excellent candidate. However, there have been few reports on incorporating multiple QDs into a single bead.<sup>2e,j,k</sup> In these cases, the photoluminescence (PL) efficiency of the QDs in the beads has been relatively low compared with their initial value. Thioglycolic acid (TGA)-capped CdTe QDs with very high PL efficiency were obtained by using an aqueous solution without post-preparative treatment when reaction conditions were optimized as we reported in previous paper.<sup>3</sup> We recently

prepared silica beads with multiple hydrophilic CdTe or ZnSe QDs that were prepared by using an inverse micelle route.<sup>4</sup> These hydrophilic QDs were incorporated without ligand (TGA) exchange on their surface. However, the detailed mechanisms on how they were incorporated and the way for the structure of the beads was controlled were not elucidated.

The structure of silica beads is another important research field. Dense nano- and micro-silica beads embedded with fluorescent monomers have been widely used as tracers in biological research.<sup>5</sup> In addition, hollow and porous silica beads have important applications in drug delivery and bio-labeling because of their structures.<sup>6a,b</sup> Extensive research has been done on synthesizing silica beads with different structures as gas and heavy-metal ion adsorbents and as inorganic carriers for bio-applications.<sup>2b</sup> Furthermore, the fabrication of silica beads with expected structures (hollow, porous, or solid) is an active research topic in materials chemistry because numerous sol–gel strategies can be utilized such as template techniques, and reaction systems can be selected.<sup>6</sup> There are two common approaches to synthesizing colloidal silica beads, namely the Stöber method and the inverse micelle route. These involve hydrolysis and the condensation of alkoxides such as tetraethyl orthosilicate (TEOS) in a solution of alcohol, water, and ammonia. The structure of silica beads can successfully be controlled when reaction procedures and conditions are properly chosen. For example, hollow silica beads were obtained by using a water/oil/water interfacial reaction without having to use any templates.<sup>6c</sup> Nann's group reported on hollow silica nanospheres fabricated by using a modified method of water-in-oil microemulsions using luminescent CdSe/ZnS

Photonics Research Institute, National Institute of Advanced Industrial Science and Technology, 1-8-31 Midorigaoka, Ikeda-city, Osaka, 563-8577, Japan. E-mail: n-murase@aist.go.jp

nanoparticles as templates.<sup>2b</sup> Lu and co-workers fabricated luminescent mesoporous silica beads under a controlled sol-gel process.<sup>7</sup> Jeong's group prepared hollow spherical silica beads with Pt nanoparticles templated by Se clusters.<sup>8</sup>

This paper presents our rate of current progress with multiple CdTe QDs embedded in a single SiO<sub>2</sub> bead by using a sol-gel technique. We found a mechanism for forming typical egg-yolk-structured (beads containing a composite) and hollow (those containing a void) beads using a controlled two-step synthesis. These beads retained relatively high PL efficiency (70%) for more than a week after they had been re-dispersed in H<sub>2</sub>O. A longer average fluorescence lifetime from the beads was found comparing with that of CdTe QDs.

## Results and discussion

### Types of beads

Table 1 lists the effects of the preparation procedures and conditions on the types of SiO<sub>2</sub> beads containing the QDs. Three kinds of beads (egg-yolk, hollow, and solid structures) were obtained. Their types strongly depended on the preparation processes (procedures A or B described in the Experimental section) and conditions, such as the ratio of Cd/TGA, their concentrations in solutions, and the pH of water phase 2 (W-2) in procedure B. Fig. 1 shows the transmission electron microscopy (TEM) photographs of SiO<sub>2</sub> beads containing the QDs prepared with procedures A or B corresponding to the different experimental conditions listed from samples 1–6 in Table 1. The structures of the three kinds of beads were clearly observed in the pictures. We found the dark area within the egg-yolk-structured beads indicated by the white arrows was a composite of Cd<sup>2+</sup>, TGA, SiO<sub>2</sub>, and QDs by using energy dispersive X-ray (EDX) analysis. In procedure A (Fig. 1(a)–(c), one water-phase injection), no hollow structures were observed. The morphology of the dark part within the egg-yolk-structured beads strongly depended on the molar ratio of Cd/TGA and their concentrations for both procedures A and B. Some solid structured beads can be observed in Fig. 1(a) whereas no solid structure beads can be observed in Fig. 1(c). The hollow beads indicated by the black arrows were obtained when procedure B (Fig. 1(d)–(f), two water-phase injections during step 2) was used. We can see dramatically different results, especially in Fig. 1(c)

(egg-yolk-structured) and Fig. 1(f) (hollow), by using procedures A and B. Therefore, the second water phase injected during the inverse micelle process (procedure B) played an important role in forming the hollow structure in the beads.

Fig. 2 shows annular dark field scanning transmission electron microscopy (ADF-STEM) photographs of SiO<sub>2</sub> beads containing the QDs (sample 4 in Table 1, *i.e.*, Fig. 1(d)). Two typical types of beads can be seen (a: a bead with a void and without a composite and b: a bead with a composite). They are denoted as hollow and egg-yolk structured, respectively. We can see clearly the distribution of the QDs within these beads. The images also show the composite (dark areas in TEM pictures) contained much more heavy ions. EDX analyses of detection points 1 and 2 are on the right in Fig. 2. The results indicated the composite contained much more Cd and S against Si. Therefore, the composite consisted of Cd<sup>2+</sup>, TGA, SiO<sub>2</sub>, and CdTe QDs. Inductively-coupled plasma (ICP) analysis of this sample revealed the molar ratio of Te/Si in whole beads was 1/79.3. According to our previous results, a green-emitting CdTe QD (2.6 nm in diameter) contained 70 Te ions.<sup>9</sup> This derived 210 Te ions for a red-emitting CdTe QD (3.9 nm in diameter). Therefore, the average concentration of these QDs in beads was calculated to be ~0.002 M. This means *ca.* 140 QDs were encapsulated into each SiO<sub>2</sub> bead 60 nm in diameter. This finding is important for applications because these beads with multiple QDs are expected to act as ultra-sensitive bio-detectors. The PL efficiency of the beads is high as explained later.

### Formation of egg-yolk-structured beads

Scheme 1 illustrates the process for forming egg-yolk-structured beads containing the QDs. Because there were Cd<sup>2+</sup> ions, TGA and SiO<sub>2</sub> monomers in the precursor solution in step 1, a composite that contained Cd<sup>2+</sup>, TGA, SiO<sub>2</sub> and QDs was formed in a water droplet during preparation. The composite grew with increasing reaction time accompanied by hydrolysis of TEOS. Furthermore, the composite migrated before solidification and shrunk after being solidified to form the egg-yolk-structure. This structure (Fig. 1(a)–(c)) strongly depended on the molar ratio of Cd/TGA and their concentrations in solutions. In our previous experiment,<sup>4b</sup> no

**Table 1** Effect of preparation procedures and conditions on types of SiO<sub>2</sub> beads containing CdTe QDs

Samples	Procedure <sup>a</sup>	Conditions			Types of beads
		Concentrations of TGA/M <sup>b</sup>	Molar ratios of Cd/TGA <sup>c</sup>	pH of W-2 <sup>d</sup>	
1	A	0.005	0.33	N/A	Egg-yolk-structured, solid
2	A	0.0025	0.33	N/A	Egg-yolk-structured, solid
3	A	0.005	0.20	N/A	Egg-yolk-structured
4	B	0.005	0.33	12.3	Hollow, egg-yolk-structured
5	B	0.0025	0.33	12.3	Hollow, egg-yolk-structured
6	B	0.005	0.20	12.3	Hollow
7	B	0.0025	0.33	10.0	Egg-yolk-structured
8	B	0.005	0.20	10.0	Solid

<sup>a</sup> Procedures A and B in Scheme 3. <sup>b</sup> Concentration in CdTe colloidal solution. <sup>c</sup> Molar ratio in CdTe colloidal solution. <sup>d</sup> pH of ammonia solutions (water-phase 2, W-2) added during inverse micelle process for procedure B.

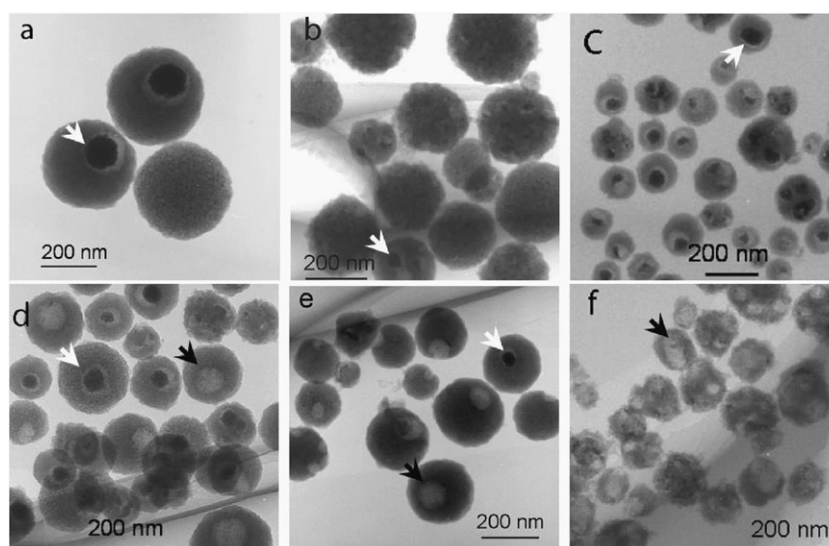


**Fig. 1** TEM photographs of SiO<sub>2</sub> beads containing CdTe QDs prepared by changing Cd/TGA molar ratio and their concentrations in colloidal solutions, (a) sample 1, (b) sample 2, (c) sample 3, (d) sample 4, (e) sample 5, (f) sample 6 in Table 1. Bead structure depended strongly on the preparation procedures, the ratio and concentration of Cd/TGA in colloidal solution. Results clearly demonstrate second water phase injection (d, e, and f) during reverse micelle synthesis resulted in formation of hollow beads while no hollow beads were observed for one water phase injection (a, b, and c). White and black arrows correspond to typical egg-yolk and hollow structures.

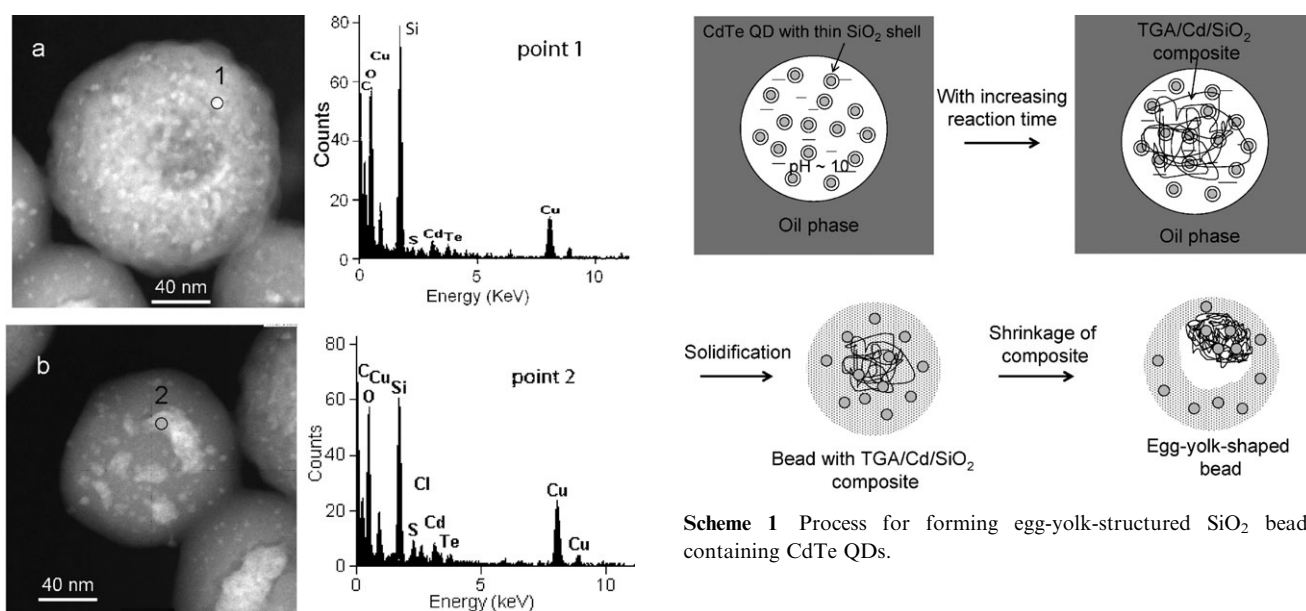


**Fig. 2** ADF-STEM photographs of SiO<sub>2</sub> beads containing CdTe QDs (sample 4 in Table 1, *i.e.*, Fig. 1(b)), (a) bead with void and without composite, (b) bead with composite of Cd/TGA/SiO<sub>2</sub>/QD. The photographs clearly show distribution of QDs in beads. EDX analysis of detection points 1 and 2 are shown on right side. Composite contained much more Cd and S.

egg-yolk-structured beads were obtained. At that time, the feeding concentration of TEOS was nearly 10-fold more than that in the current experiments. This means the feeding concentration of TEOS during step 1 is another important factor in forming this structure.

A previous publication has reported a one-dimensional chain-like structure formed by cadmium ions and various types of thiol ligands has been found in the microcrystals of

cadmium coordination polymers.<sup>10</sup> Cd-TGA complexes with different morphologies were formed under reflux in an aqueous solution of Cd<sup>2+</sup>, TGA, and poly(acrylic acid) sodium salt (PAA) by changing the molar ratio of Cd/TGA.<sup>11</sup> In that case, nanowires were formed by the complex of Cd<sup>2+</sup> and TGA after connection to PAA. It is known that Cd<sup>2+</sup> and TGA can form chains in an aqueous solution under alkaline conditions because of the connection between mercapto groups and Cd<sup>2+</sup> ions. The formation of these chains strongly depends on the ratio of Cd/TGA and their concentration in solution. Because the entire reaction time for the current experiment lasted more than one day, Cd<sup>2+</sup> ions and TGA first connected to form their chains. SiO<sub>2</sub> monomer is then connected with these Cd-TGA chains to form a Cd/TGA/SiO<sub>2</sub> composite, which is similar to a



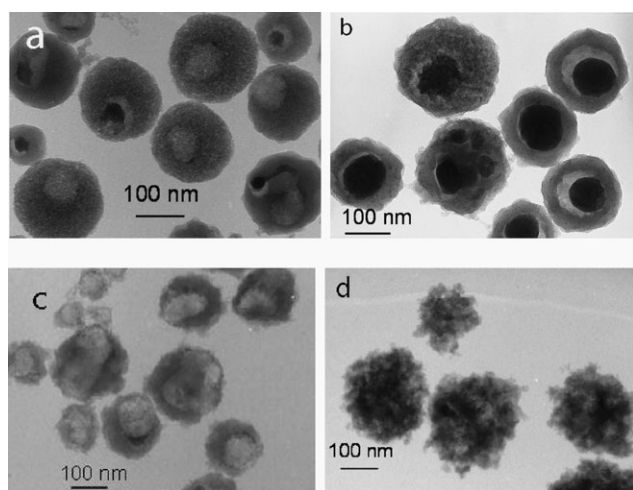


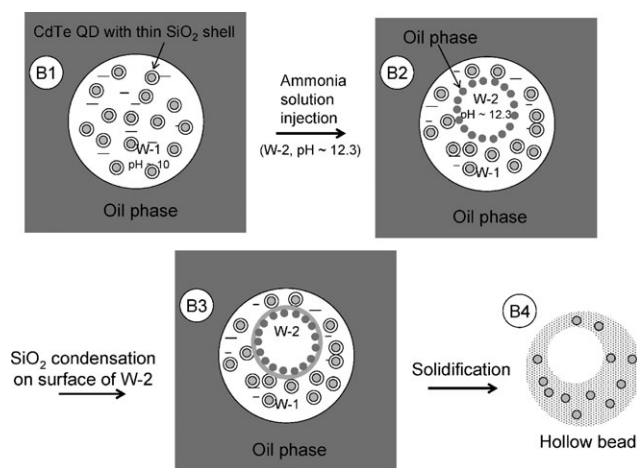
**Fig. 3** TEM photographs of SiO<sub>2</sub> beads containing CdTe QDs using procedure B with W-2 (ammonia solution) with different pH: (a) sample 5 (pH ~12.3), (b) sample 7 (pH ~10), (c) sample 6 (pH ~12.3), (d) sample 8 (pH ~10). Hollow beads were obtained due to high pH (~12.3) of W-2.

Cd/TGA/PAA composite.<sup>11</sup> The CdTe QDs were assembled into these composites during preparation because they have a thin SiO<sub>2</sub> layer on the surface. Additionally, because the composite is a gel at the beginning, it shrinks significantly after solidification. This resulted in the formation of egg-yolk-structured beads. Since the hydrolysis and condensation of TEOS strongly depend on the pH of the solution, the pH affects the formation of the composite, as explained below in Fig. 3.

### Formation of hollow-structured beads

A typical strategy for producing hollow silica beads is removing templates by heating or by using other chemical treatment. Organic spheres, oil droplets, and aggregates of polymer or surfactant are often used as templates. The preparation of hollow SiO<sub>2</sub> beads without a template has also been examined recently.<sup>6c</sup> The chemistry of sol–gel silica has provided ideal approaches to fabricating these silica materials with required design structures by changing the reaction system and conditions. Here, we successfully prepared hollow SiO<sub>2</sub> beads with multiple CdTe QDs by controlling the condensation of SiO<sub>2</sub> monomers on the surface of a small droplet of an ammonia solution taken in the SiO<sub>2</sub> beads as explained later.

Scheme 2 shows the process for forming the hollow SiO<sub>2</sub> beads containing the QDs. The second smaller water droplet with a highly alkaline condition (pH ~12.3) from the ammonia solution taken in the water droplet played an important role in forming this hollow structure in beads. For procedure B, the precursor solution (water phase 1, W-1, pH ~10) was first injected into the stock solution to form a microemulsion. After that, the ammonia solution (W-2, pH ~12.3) was injected into the microemulsion. Immediately after the W-2 had been injected, small droplets of the ammonia solution were formed in the microemulsion. Cyclohexane molecules were attached outside the surfactant



**Scheme 2** Process for forming hollow SiO<sub>2</sub> beads containing CdTe QDs: B1–B4 correspond to the positions of preparation process shown in Scheme 3.

located on the small droplets. With increasing reaction time, these small droplets were taken into the W-1. The condensation of SiO<sub>2</sub> monomers occurred quickly on the surface of the small droplets because of the higher pH (~12.3) similar to a mechanism described elsewhere.<sup>6c</sup> The small droplets developed into hollow structures. When the pH of droplets was the same as that of the precursor solution (W-1, pH 10), quick condensation by SiO<sub>2</sub> monomers did not occur. As a result, the small droplets of ammonia solution mixed with W-1 to form a homogeneous water phase. Therefore, no hollow structures were formed in these beads, as will be explained later in more detail.

To prove that pH had an influence on the structure of hollow beads, Fig. 3 shows the TEM photographs of SiO<sub>2</sub> beads containing the QDs prepared by procedure B, in which W-2 with different pH were used ((a) sample 5 (pH ~12.3), (b) sample 7 (pH ~10), (c) sample 6 (pH ~12.3) and (d) sample 8 (pH ~10)). The details on the preparation procedures and conditions for all samples are listed in Table 1. With a high pH (~12.3), hollow-structured beads were obtained (Fig. 3(a) and (c)), while egg-yolk-structured (Fig. 3(b)) and solid (Fig. 3(d)) beads were observed when W-1 and W-2 had the same pH (~10). The mechanism shown here can be used to incorporate another component such as magnetic nanocrystals in the hollow space to give an additional function to PL.

### Luminescence of beads

Fig. 4(a) shows the absorption and PL spectra of SiO<sub>2</sub> beads containing the QDs (sample 4 in Table 1, under a 0.45-μm filter) in H<sub>2</sub>O and the scanning electron microscopy (SEM) photograph is shown in Fig. 4(b). The PL efficiency of the QDs within these beads in water was 70%, which is very close to their initial value. These beads also retained their high PL efficiency in water for more than a week. These results indicated the current method of preparation is excellent because silica can be coated on the QDs while still retaining their initial surface conditions. This contributed to retaining their initial PL efficiency even when several procedures were

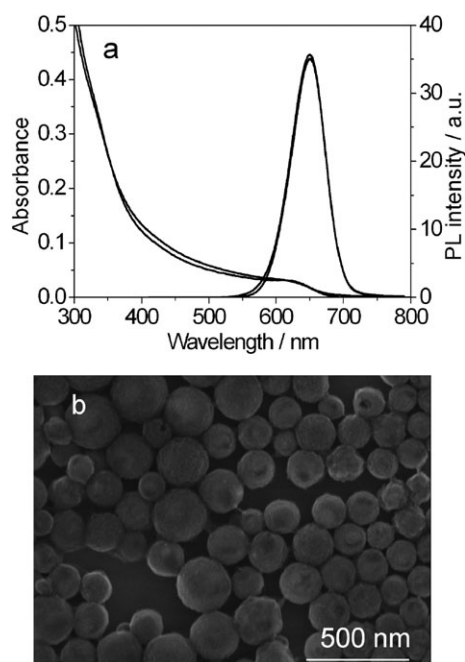


**Fig. 4** Absorption and PL spectra (a) and SEM photograph (b) of SiO<sub>2</sub> beads containing CdTe QDs (sample 4 in Table 1, grey line) in H<sub>2</sub>O. Absorption and PL spectra (black line) of a CdTe colloidal solution are shown for comparison. PL efficiency of CdTe QDs in beads was 70% while their initial value in colloidal solution was 72%.

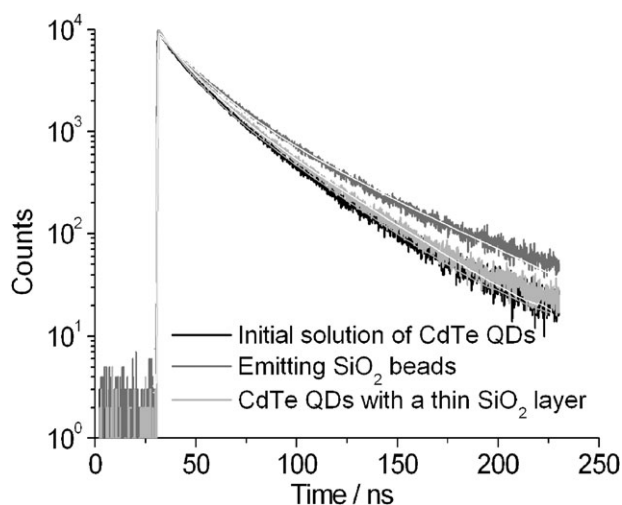


**Fig. 5** Luminescence decay curves (measured on the emission peak maximum,  $\lambda_{\text{ex}} = 374$  nm) of emitting SiO<sub>2</sub> beads (sample 4 in Table 1, grey line), CdTe QDs coated with a thin SiO<sub>2</sub> layer by step 1 (light grey line), and initial solution of CdTe QDs (black line). Reproduced curves using the values shown in Table 2 are plotted as thin white lines.

used in processing including bead separation. Other samples revealed similar PL properties (PL efficiency, the peak position and width of PL spectra) to those of sample 4. This means all kinds of beads retained high PL efficiencies under current experimental conditions.

Fig. 5 shows the luminescence decay curves (measured on the emission peak maximum,  $\lambda_{\text{ex}} = 374$  nm) of emitting SiO<sub>2</sub> beads, CdTe QDs coated with a thin SiO<sub>2</sub> layer by step 1, and the initial solution of CdTe QDs. The decay curves can be well fitted to a biexponential model described by  $F(t) = A + B_1 \exp(-t/\tau_1) + B_2 \exp(-t/\tau_2)$ , where  $\tau_1$  and  $\tau_2$  represent the time constants and  $B_1$  and  $B_2$  represent the amplitudes of the components, respectively. The average lifetime  $\tau$  is calculated by an expression  $\tau = (B_1 \tau_1^2 + B_2 \tau_2^2) / (B_1 \tau_1 + B_2 \tau_2)$ .<sup>12</sup> The fitting parameters  $B_1$ ,  $B_2$ ,  $\tau_1$ ,  $\tau_2$ , and  $\tau$  are summarized in Table 2. It is noted that the fast component of the PL decay in bare CdTe QDs can be associated with an exciton recombination.<sup>13</sup> The slow component is considered to originate from the surface-related emission of CdTe QDs. Comparing with CdTe QDs, the fast component ( $B_1$ ) of PL decay for the bead increased while the slow component ( $B_2$ ) decreased. The average PL decay lifetime of 27.7 ns for CdTe QDs was increased to 29.6 ns after coating with a thin SiO<sub>2</sub> shell on their surface by step 1. In addition, the average PL decay lifetime of 27.7 ns was found to increase further to 38.7 ns after encapsulating the QDs in beads. According to the calculation shown in literature,<sup>12b</sup> this successive increment is accompanied by the reduction of non-radiative decay rate. These tendencies are ascribed to the surface modification of CdTe QDs due to the SiO<sub>2</sub> coating.

## Conclusions

We prepared two types of SiO<sub>2</sub> beads (hollow and egg-yolk structured) with multiple CdTe QDs using a two-step synthesis by controlling the preparation procedures and conditions. On the one hand, we devised a method of control to obtain a hollow structure through injecting a second water phase with a high pH ( $\sim 12.3$ ) during the inverse micelle process. The hollow structure thus formed indicated that we could encapsulate other materials (such as magnetic nanoparticles and drug molecules) within beads at the same time to give the beads several functions. On the other hand, we prepared egg-yolk-structured beads that contained a composite made up of Cd/TGA/SiO<sub>2</sub>/QDs, by adjusting the experimental parameters and selecting the preparation procedures. Their formation mechanism was discussed as well. Furthermore, these beads exhibited good stability and high PL efficiency in water. The average luminescence lifetime of CdTe QDs and emitting SiO<sub>2</sub> beads are 27.7 and 38.7 ns, respectively.

**Table 2** Time constants  $\tau_1$  and  $\tau_2$ , components  $B_1$  and  $B_2$ , average lifetime  $\tau$ , and PL efficiency  $\eta$  of as-prepared CdTe QDs in water, those coated with thin SiO<sub>2</sub> layer by step 1, and those incorporated into SiO<sub>2</sub> beads (sample 4 in Table 1)

Sample	$\eta$ (%)	$B_1$ (%)	$\tau_1$ /ns	$B_2$ (%)	$\tau_2$ /ns	$\tau$ /ns
QDs	72	32.1	10.9	67.9	30.5	27.7
After step 1	72	36.4	12.8	63.6	33.3	29.6
Beads	70	48.2	17.3	58.2	45.5	38.7

Together with the PL efficiency data, this indicates the reduction of non-radiative rate and increment of radiative lifetime of the QDs by SiO<sub>2</sub> coating. The high PL efficiency (70% in H<sub>2</sub>O) from multiple CdTe QDs in each bead would be extremely practical for ultra-sensitive bio-probes.

## Experimental

### CdTe QDs and chemicals

TGA-capped CdTe QDs in an aqueous solution were prepared with a procedure using cadmium perchlorate and hydrogen telluride, as described in a previous paper.<sup>3</sup> The PL efficiency of the QDs in colloidal solutions was 72% for the red-emitting QDs. All chemicals used were of analytical grade or of the highest purity available. The pure water was from a Milli-Q synthesis system.

### Preparation of beads

SiO<sub>2</sub> beads containing dispersed CdTe QDs were prepared by using a two-step synthesis (step 1: coating the QDs with a thin SiO<sub>2</sub> layer and step 2: encapsulating these SiO<sub>2</sub>-coated QDs into glass beads) referring to a previous method.<sup>4b</sup> In the current experiments, the QDs were re-dispersed in a solution of Cd<sup>2+</sup> (Cd(ClO<sub>4</sub>)<sub>2</sub>) and TGA after adjusting the ratio of Cd/TGA and their concentrations before the beads were prepared. The pH of the solution of Cd<sup>2+</sup> and TGA was retained at 10 by using an NaOH solution. The feeding concentration of TEOS during step 1 was also optimized with the joint aims of controlling the structure and the size of the beads briefly as follows.

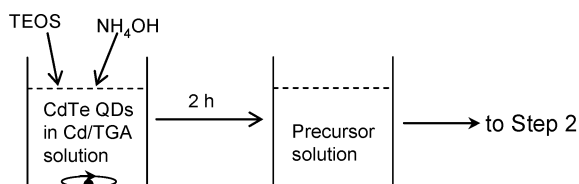
A re-dispersed CdTe colloidal solution (2 mL,  $2.2 \times 10^{-6}$  M), a diluted ammonia solution (50  $\mu$ L, 6.25 wt%), and TEOS (20  $\mu$ L) were mixed in a vial with a cover for 2 h to obtain the precursor solution for the CdTe QDs coated with a thin SiO<sub>2</sub> layer (step 1). For step 2, Igepal CO-520 (3.52 g) was added to cyclohexane (25 g) while stirring until the solution became clear to obtain the stock solution. For procedure A in Scheme 3, an ammonia solution (100  $\mu$ L, 6.25 wt%) was first added into the precursor solution and mixed for 10 min while stirring. The as-prepared solution ( $\sim 2$  mL) was then injected into the stock solution drop-by-drop to prepare a microemulsion while vigorously stirring. For procedure B in Scheme 3, the precursor solution (water phase 1 (W-1),  $\sim 2$  mL) was first injected into the stock solution drop-by-drop to prepare the microemulsion while vigorously stirring. An ammonia solution (water phase 2 (W-2), 6.25 wt%, pH  $\sim 12.3$ , 100  $\mu$ L) was then injected dropwise. Normally, the reaction time during step 2 was 24 h. The molar ratio of Cd/TGA and their concentrations were selected when the CdTe QDs were being re-dispersed to find what dependence the structure of the beads had on the experimental conditions.

### Apparatus

SEM photographs of samples were taken with a Hitachi S-5000 field emission scanning electron microscope. Observations by TEM and ADF-STEM and analysis by EDX were carried out on Hitachi H-9000NA (300 kV) or FEI Tecnai G2 F20 (200 kV) electron microscopes. To prepare TEM or SEM specimens, as-prepared microemulsion was filtered through a 0.45- $\mu$ m filter to remove the large beads. This microemulsion was then centrifuged at 22 000 rpm for

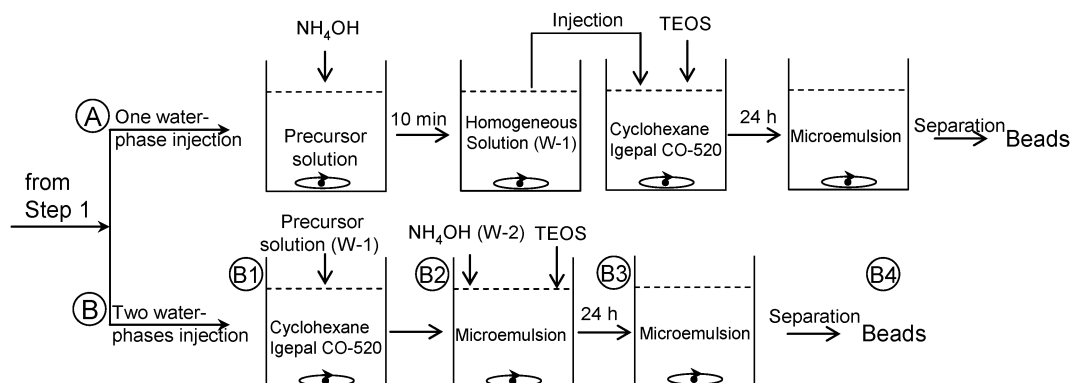
#### Step 1

#### Coating CdTe QDs with thin SiO<sub>2</sub> layer



#### Step 2 (two kinds of synthesis procedures)

#### Encapsulation of the SiO<sub>2</sub>-coated CdTe QDs in glass beads



Scheme 3 Typical preparation process for SiO<sub>2</sub> beads containing CdTe QDs by using two-step synthesis.

30 min to obtain a powder sample which was washed three times with ethanol. The molar ratio of Te/Cd/Si in the beads was measured with an ICP spectrometer (SPS4000, SII Nanotechnology Inc.).

The absorption and PL spectra were taken using conventional spectrometers (Hitachi U-4000 and F-4500). The PL efficiencies of the emitting beads and CdTe QDs in solutions were estimated with a method previously reported.<sup>14</sup> Briefly, the dependence of PL intensity on absorbance was compared with a standard solution (quinine sulfate in 0.05 M H<sub>2</sub>SO<sub>4</sub>). Fluorescence lifetimes were measured using time-correlated single photon counting spectrofluorimeter systems (FluoroCube-3000U, Horiba). The recorded decay curves were fitted with a multi-exponential function deconvoluted with system response.

## Acknowledgements

This study was supported in part by the Creation and Support Program for Start-ups from Universities, sponsored by the Japan Science and Technology Agency (JST). Dr Yang is also grateful to the Research Fellowship of the Japan Society for the Promotion of Science (JSPS).

## References

- W. C. W. Chan and S. Nie, *Science*, 1998, **281**, 2016; M. Bruchez, Jr, M. Moronne, P. Gin, S. Weiss and A. P. Alivisatos, *Science*, 1998, **281**, 2013.
- (a) Z. Zhelev, H. Ohba and R. Bakalova, *J. Am. Chem. Soc.*, 2006, **128**, 6324; (b) M. Darbandi, R. Thomann and T. Nann, *Chem. Mater.*, 2007, **19**, 1700; (c) K. Iwasaki, T. Torimoto, T. Shibayama, H. Takahashi and B. Ohtani, *J. Phys. Chem. B*, 2004, **108**, 11946; (d) Z. Lu, J. Dai, X. Song, G. Wang and W. Yang, *Colloids Surf., A*, 2008, **317**, 450; (e) Y. Yang and M. Gao, *Adv. Mater.*, 2005, **17**, 2354; (f) Y. Yang, L. Jing, X. Yu, D. Yan and M. Gao, *Chem. Mater.*, 2007, **19**, 4123; (g) T. T. Tan, S. T. Selvan, L. Zhao, S. Gao and J. Y. Ying, *Chem. Mater.*, 2007, **19**, 3112; (h) H. Li and F. Qu, *Chem. Mater.*, 2007, **19**, 4148; (i) X. Gao and S. Nie, *J. Phys. Chem. B*, 2003, **107**, 11575; (j) R. Koole, M. M. Schooneveld, J. Hilhorst, C. M. Donegá, D. C. Hart, A. Blaaderen, D. Vanmaekelbergh and A. Meijerink, *Chem. Mater.*, 2008, **20**, 2503; (k) A. L. Rogach, D. Nagesha, J. W. Ostrander, M. Giersig and N. A. Kotov, *Chem. Mater.*, 2000, **12**, 2676.
- C. L. Li and N. Murase, *Chem. Lett.*, 2005, **34**, 92.
- (a) S. T. Selvan, C. L. Li, M. Ando and N. Murase, *Chem. Lett.*, 2004, **33**, 434; (b) P. Yang, M. Ando and N. Murase, *J. Colloid. Interface Sci.*, 2007, **316**, 420; (c) M. Ando, C. L. Li, P. Yang and N. Murase, *J. Biomed. Biotechnol.*, 2007, ID52971.
- (a) B. Zhang, E. T. Bergström, D. M. Goodall and P. Myers, *Anal. Chem.*, 2007, **79**, 9229; (b) T. R. Sathe, A. Agrawal and S. Nie, *Anal. Chem.*, 2006, **78**, 5627; (c) X. Gao and S. Nie, *Anal. Chem.*, 2004, **76**, 2406.
- (a) I. I. Slowing, B. G. Trewyn, S. Giri and V. S. Y. Lin, *Adv. Funct. Mater.*, 2007, **17**, 1225; (b) C. Wu, J. Zheng, C. Huang, J. Lai, S. Li, C. Chen and Y. Zhao, *Angew. Chem., Int. Ed.*, 2007, **46**, 5393; (c) M. Fujiwara, K. Shiokawa, Y. Tanaka and Y. Nakahara, *Chem. Mater.*, 2004, **16**, 5420; (d) A. P. R. Johnston, B. J. Battersby, G. A. Lawrie and M. Trau, *Chem. Commun.*, 2005, 848.
- J. Lu, M. Liong, J. I. Zink and F. Tamanoi, *Small*, 2007, **3**, 1341.
- G. D. Moon, U. Jeong and Y. Xia, *Chem. Mater.*, 2008, **20**, 367.
- N. Murase, N. Gaponik and H. Weller, *Nanoscale Res. Lett.*, 2007, **2**, 230.
- I. G. Dance, M. L. Scudder and R. Secomb, *Inorg. Chem.*, 1983, **22**, 1794.
- H. Niu and M. Gao, *Angew. Chem., Int. Ed.*, 2006, **45**, 6462.
- (a) R. Osovsky, V. Kloper, J. Kolny-Olesiak, A. Sashchiuk and E. Lifshitz, *J. Phys. Chem. C*, 2007, **111**, 10841; (b) Q. Zeng, X. Kong, Y. Sun, Y. Zhang, L. Tu, J. Zhao and H. Zhang, *J. Phys. Chem. C*, 2008, **112**, 8587.
- S. F. Wuister, F. v. Driel and A. Meijerink, *Phys. Chem. Chem. Phys.*, 2003, **5**, 1253.
- N. Murase and C. L. Li, *J. Lumin.*, 2008, **128**, 1896.